Optical elements based on silicon photonics

M.A. Butt[1], E.S. Kozlova[1,2]

[1]Samara National Research University, Moskovkoye Shosse 34, Samara, Russia, 443086
[2]Image Processing Systems Institute of RAS - Branch of the FSRC "Crystallography and Photonics" RAS, Molodogvardejskaya street 151, Samara, Russia, 443001

Abstract. Silicon photonics is gaining substantial impulse because it permits optical devices to be realized inexpensively using standard semiconductor fabrication techniques and integrated with microelectronic chips. In this paper, we proposed some optical elements based on silicon platform simulated using Finite Element Method (FEM).

1. Introduction

Silicon photonics can be dated back to the 1980s. Nevertheless, the previous era has observed an unexpected growth in the field. Based on exceedingly advance silicon semiconductor technology, silicon photonics would deliver with a low-cost, highly integrated electronic-photonic platform, in which ultra-compact photonic devices and electronic circuits are united. The ultimate motive behind silicon photonics is the ability to use CMOS-like fabrication resulting in high volume production at low cost [1]. In this paper, we designed optical power splitter, Bragg gratings and polarization beam splitter based on silicon platform. All the simulations are performed by using Comsol Multiphysics 5.1 which solves the Helmholtz equation with the finite element method (FEM).

2. Optical power splitter

Optical power splitters (OPS) play an important role in optical communication systems [2] and periodic optical sources for integrated microfluidic devices. OPSs are mainly based on either Y-branch splitters [3] or multimode interference (MMI) splitters. In this paper, we modelled 1×4 OPS 8 μm long based on coupled- mode theory (CMT) [4] by using seven vertically slotted waveguides at 1550 nm TE-polarized light. Numerical optimizations were performed on the coupling gap (C1, C2 and C3) between the slot waveguides structures (by keeping the coupling lengths constant) in order to achieve an equal power distribution among 4 outputs. The CMT is used to evaluate the mode coupling or conversion in optical waveguides. The physical models for coupled waveguide systems contain two or more dielectric waveguides engaged in close vicinity. These waveguides may be parallel to each other or may have variable separations. The splitter schematic structure is shown in fig 1. And the slot waveguide cross section is described by the inset. The coupling strength is very sensitive to the distance between the WGs and it is important to eventually pick a design that can function effectively given the type of deficiencies that are expected from the manufacturing process.

In the first stage, $C1$ is varied from 30 – 200 nm between WG1 and the adjacent WGs (2 and 3). The coupling efficiency of $C1$ is plotted in fig. 2 a). It can be seen that when $C1 < 45$ nm, the energy doesn't transfer to the adjacent WGs instead it confines itself in $C1$. This happens because the gap is too small that it behaves as another slot WG and tries to confine the energy in $C1$.

A maximum coupling efficiency is obtained at values between 90 – 125 nm where the power is equally divided between WG2 and WG3 with less coupling losses. Hence, we used a finest value of *C*1 = 115 nm in our splitter design for maximum coupling. Based on these results, *C*2 is also fixed at 115 nm to acquire maximum coupling between WGs (2, 3) and WGs (4, 5). In order to obtain the balanced 1×4 OPS, *C3* has to be slightly adjusted. The distribution of the power between WG3 and WG7 is not equal as seen in fig. 2 b) where normalized intensity distribution at port 1, port 2, port 3 and port 4 are shown for various values of C3. For values of C3 < 140 nm, the output intensity at Port 2 and Port 3 is less than Port 1 and Port 4. The optimized value of C3 is obtained at 140 nm where the OPS is balanced with 25 % of power transmission at each port as shown in fig. 2 b). The line graph at Port 1, Port 2, Port 3 and Port 4 is shown in fig. 2c.

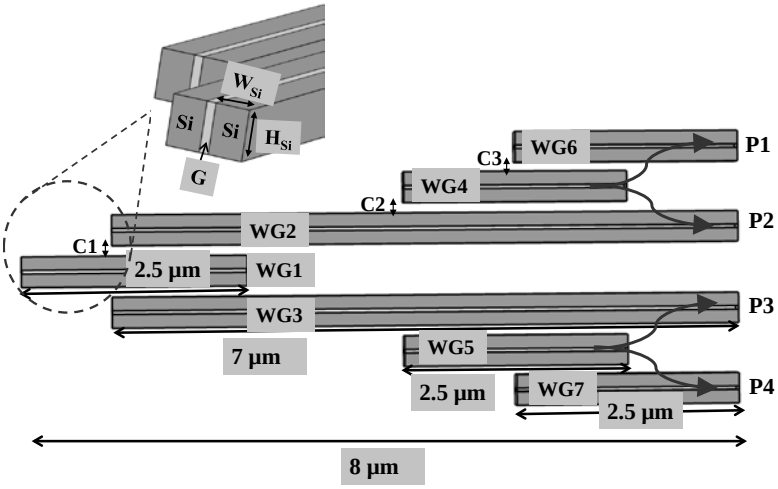

Figure 1. Schematic of a 1x4 OPS.

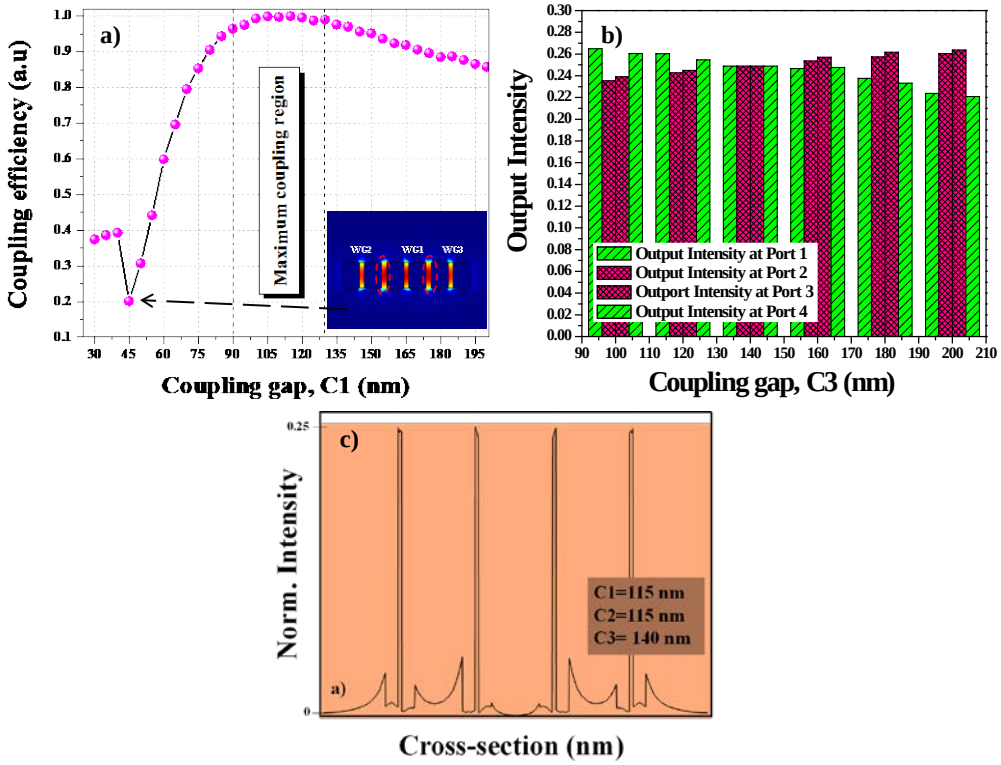

Figure 2. a) Coupling efficiency C1 vs coupling gap, b) Coupling gap, C3 versus intensity distribution at port 1, port 2, port 3 and port 4, c) Normalized intensity at Port 1, Port 2, Port 3 and Port 4.

3. Polarization Beam Splitter

A polarization beam splitter (PBS) is one of the most important components in modern optical communication systems and is used to separate the two orthogonal polarizations of light. The working principle of conventional PBS devices is based on either modal evolution [5] or interferometry. Numerous devices such as multimode interference couplers, directional couplers (DCs) and Mach–Zehnder interferometers are based on the principle of interferometry. Among these, PBS devices based on DCs are preferred because they are generally compact in size. In this paper, we propose a fairly simple and compact PBS design based on two strip WGs separated by a Bridge WG as shown in figure 3. L1 = L2 = 12 μm, which is the length of WG1 and WG2. Light with either polarization TE/TM is coupled at WG1 (input WG). TE-polarized light is collected from WG1 whereas TM-polarized light is coupled through a Bridge WG and collected at WG2.

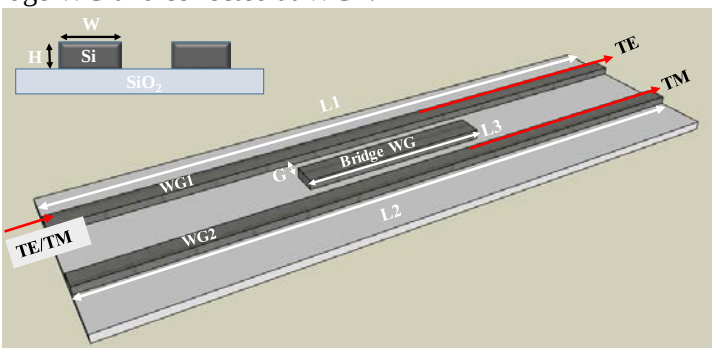

Figure 3. Schematic of a PBS.

Si WGs have large polarization mode dispersion (PMD) owing to their structural birefringence. That is why there is a significant difference in the coupling lengths between the two polarization modes due to the different propagation constant initiated by the PMD. When a TM-polarized light is coupled into WG1, the light beam is transferred to WG2 after propagating through a coupling length. As a substitute, the TE-polarized light usually has a longer coupling length than the TM-polarized light does, therefore the TE-polarized light travels in the same WG, without crossing to the other WG, after propagating through the same coupling length. In our design, the coupling efficiency of the TM-mode intensely depends on the length of the bridge WG (L_{BWG}). We present the contour plot of the TM-mode at the output of the PBS (figures 4(a)–(d)).

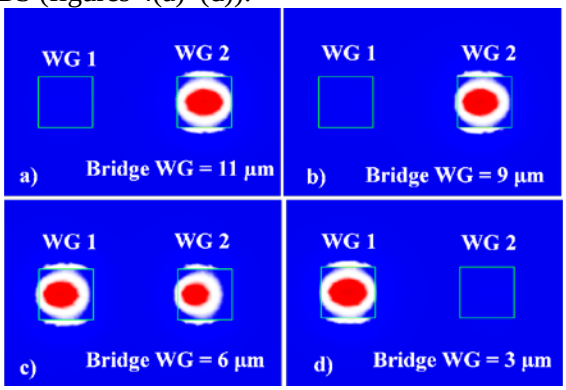

Figure 4. Contour plot of TM mode at the output of PBS.

The L_{BWG} varies from 2 to 11 μm with a step size of 1 μm. When $L_{BWG} \geqslant 9$ μm, the TM-mode has a maximum coupling efficiency, as shown in figures 4 (a) and (b). At $L_{BWG} = 6$ μm, the design acts as a power divider for the TM polarization only as shown in figure 4 (c); at $L_{BWG} = 3$ μm, no coupling of the TM-mode takes place as shown in figure 4 (d). The amount of power coupled is decided by the overlap of the modes in the separate channels. Thus, it depends on the WG's separation (G) and the interaction length (L_{BWG}). The value of G between the WGs plays an important role in the coupling of the TM-mode from WG1 to WG2 while also maintaining the TE-mode in WG1. We keep the value of

G identical between the WG1-Bridge WG and the Bridge WG-WG2. The mode power of TE and TM was calculated at 1550 nm in WG1 and WG2, respectively, for *G* varies between 50–150 nm. At $G < 50$ nm, the mode power of both TE/TM polarizations in the WGs is inconsiderable because the light is mostly confined to the *G*. The maximum value of the TE- and TM-modes was obtained at $G = 150$ and 120 nm, respectively. So there is a slight compromise in selecting the optimum value of *G* where both the modes can have high values. Hence, for our PBS design, we choose $G = 120$ nm where both polarizations have more than 70% mode power, as shown in figure 5.

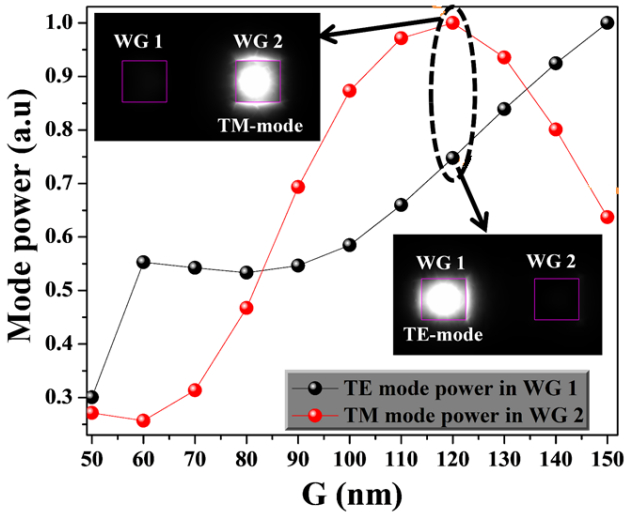

Figure 5. Mode power vs coupling gap (G).

4. Bragg grating

Bragg gratings (BG) are optical elements with spatially, periodically varying refractive indices. They are not only used in telecommunication but also extensively used as temperature, strain, pressure, current and (bio) chemical sensors [6]. Bragg gratings can be incorporated into planar WG structures at a high integration density. Bragg gratings back-reflect a certain wavelength within the WG instead of coupling it in or out such as grating couplers. We designed a Fabry Perot resonator based on silicon slot WG. In slot WG, the guided light is strongly confined within a narrow low-index slot (S) between the two high indices photonic wires [7]. There are two claddings (high index material). In our design, we are considering air (n=1) as a slot and Si (n=3.45) as a high index material. The electric field propagating in the slot go through an interference at the high contrast interface which makes the electromagnetic wave to confine intensely in the narrow slot than in the cladding. This leads to the implementation of compact and high-performance photonic components such as resonators and polarization beam splitters. The width and height of a silicon slot WG are denoted as W_a and H_a, respectively. The width of the slot is S as shown in figure 6.

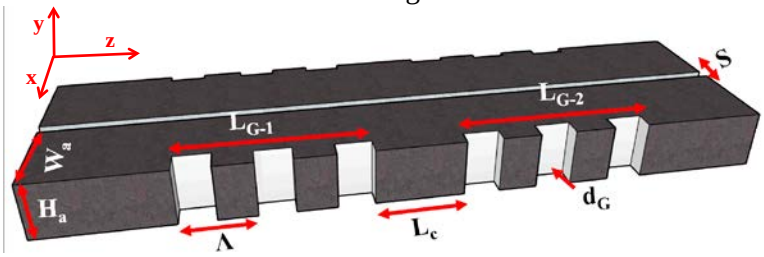

Figure 6. Schematic of a Bragg gratings and cavity on both sides of the silicon slot WG.

The transmission spectrum of the *FP*-resonator based on slot WG is demonstrated for N_G=20 and 30 by maintaining the d_G=30 nm as shown in figure 7. It is observed that, the *FWHM* and *FSR* is about 3.1 nm and 43 nm, respectively for N_G=20. Whereas, for N_G= 30, the *FWHM* and *FSR* is around 2.1 nm and 34 nm, respectively. This clearly indicates that, we can control the spectral characteristics by manipulating the number of grating periods.

The electric field distribution of *FP*-resonator for N_G=30 is plotted in figure 8. The varying transmission function of a *FP*-resonator is produced due to the interference between the multiple reflections of light between two DBRs. If the transmitted beams are out of phase then destructive interference takes place which corresponds to a minimum or zero transmission as shown in figure 8 a). Whereas if the transmitted beams are in phase then constructive inference occurs and this delivers a high transmission peak of the resonator as demonstrated in figure 8 b).

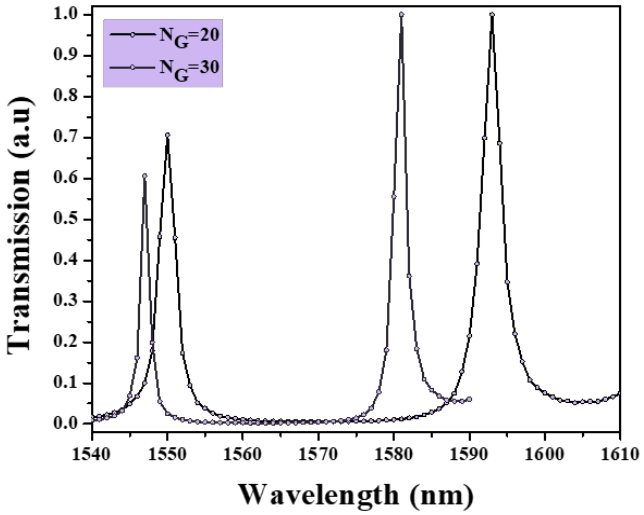

Figure 7. Transmission spectrum of a *FP*-resonator for N_G=20 and 30, where H_a=0.22 μm, W_a=0.27 μm, S= 50 nm, L_c= 0.5 μm, d_G=30nm.

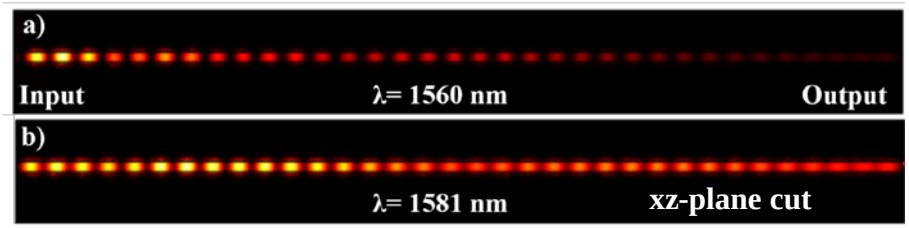

Figure 8. The Electric field distribution, a) the *xz*-plane at H_a/2 for 1560 nm, b) *xz*-plane cut at H_a/2 for 1581 nm.

5. Conclusion

In this work we proposed several optical elements such as optical power splitter, bragg grating and polarization beam splitter based on silicon photonics. These results can provide the guidelines for the fabrication of numerous other devices using silicon photonic technology.

6. References

[1] Bogaerts, W. Nanophotonic waveguides in silicon-on-insulator fabricated with CMOS technology / W. Bogaerts, R. Baets, R. Dumon, V. Wiaux, S. Beckx, D. Taillaert, B. Luyssaert, J. V. Campenhout, P. Bienstman, D. V. Thourhout // J. Lightw. Technol. – 2005. – Vol. 23(1). – P. 401-412.

[2] Butt, M.A. A compact design of a balanced 1x4 optical power splitter based on silicon on insulator slot waveguides / M.A. Butt, S.N. Khonina, A.N.K. Reddy // Computer Optics. – 2018. – Vol. 42(2). – P. 244-247. DOI: 10.18287/2412-6179-2018-42-2-244-247.

[3] Butt, M.A. Fabrication of Y-splitters and Mach Zehnder structures on (Yb,Nb):$RbTiOPO_4$/$RbTiOPO_4$ epitaxial layers by reactive ion etching / M.A. Butt, R. Sole, M.C: Pujol, A. Rodenas, G. Lifante, A. Choudhary, G.S. Murugan, D.P. Shepherd, J.S. Wilkinson, M. Aguilo, F. Diaz // J. Lightw. Technol. – 2015. – Vol 33(9). – P. 1863-1871.

[4] Huang, W.P. Coupled mode theory for optical waveguides: an overview / W.P. Huang // JOSA A. – 1994. – Vol 11(3). – P. 963-983.

[5] Watts, M.R. Integrated mode evolution based polarization splitter / M.R. Watts, H.A. Haus, E.P. Ippen // Opt. Lett. – 2005. – Vol 30(9). – P. 967-969.
[6] Lee, B. Review of the present status of optical fiber sensors / B. Lee // Opti. Fiber Technol. – 2003. – Vol 9(2). – P. 57-59.
[7] Butt, M.A. Silicon on silicon dioxide slot waveguide evanescent field gas absorption sensor / M.A. Butt, S.N. Khonina, N.L. Kazanskiy // J. Mod. Opt. – 2018. – Vol 65(2). – P. 174-178.

Acknowledgments
This work was partly funded by the RF Ministry of Science and Higher Education within the state project of the FSRC “Crystallography and Photonics” RAS under agreement 007-GZ/Ch3363/26 (“Optical power splitter”) and the Russian Foundation for Basic Research under projects ## 18-07-01122 ("Polarization Beam Splitter"), 18-07-01380 (“Bragg grating").